Measurements on the Frequency Entrainment of a Reflex Klystron

By

Jun-ichi IKENOUE* and Kiyoshi FUKUI*

(Received October 31, 1960)

The bandwidth of frequency entrainment of a reflex klystron was measured in relation to the power ratio of an applied external signal and the output of of the klystron at its normal operation. Measurements were also carried out on the output power of a frequency-entrained reflex klystron both for the various frequency deviations of signal frequency from that of the klystron at its normal operation and for the various power ratios.

As a supplement to the theory previously reported by the authors, an analysis is given for the case when the klystron does not operate at the center of an electronic mode in the absence of an external signal. It is shown that the theory is in rather good agreement with the experimental results.

1. Introduction

The phenomenon of frequency entrainment in a reflex klystron is, so to speak, the microwave analogue of the entrainment in an ordinary vacuum tube oscillator, and a theoretical analysis of it was given first by Slater[1] and more recently by the authors[2]. It was shown in our previous paper that under conditions such that the oscillator runs under a matched load at normal operation with no electronic susceptance, the electronic susceptance does not change appreciably due to entrainment. Furthermore, the frequency of oscillation of the klystron cavity shifts to the frequency of an applied signal, so that the effectively added susceptance due to the signal may be counterbalanced by the change in susceptance of the resonant cavity. This statement would receive further support if certain predictions of the theory, such as the one for the bandwidth of frequency entrainment, were experimentally observed.

The purpose of this paper is to present some experimental results on the characteristics of a frequency-entrained reflex klystron and to compare them with the theory which was developed chiefly in the previous paper but is supplemented here. It should be noted that the experiment presented here is concerned with the static aspect of the phenomenon, and that the dynamic aspects, such as the time lag of entrainment, will be the subject of future studies.

* Department of Electronics

2. Method and Apparatus

Among the various circuit arrangements which enable us to observe the entrainment phenomenon of a reflex klystron, we employed the one shown in Fig. 1. In accordance with the basic assumption of the theory, the reflex klystron under test was adjusted to operate under a matched load at the center of an electronic mode before the application of an external signal. The T-junction II was also adjusted in such a way that no reflection occurred for the wave entering from the branch waveguide in the frequency range concerned. The signal power

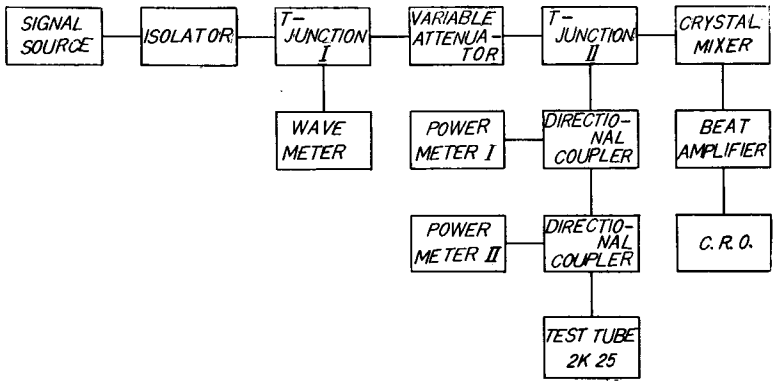

Fig. 1. Block diagram of the apparatus.

fed into the test tube could be varied continuously through the variable attenuator and was measured by the power meter I. When the test tube is not entrained by the signal, beats should occur at the crystal mixer and we could observe them on the C.R.O. But if no beats are observed, we may consider the system entrained. Using the apparatus of Fig. 1, measurements could be made on the bandwidth of the frequency entrainment and on the output power of the entrained system.

3. Bandwidth of Frequency Entrainment

Let the signal power be increased from zero value. As the magnitude of the signal power reaches that value necessary for entrainment, the beats suddenly disappear. This value depends on the frequency deviation of the signal frequency, $p/2\pi$, from that of the test tube at its normal operation, $\omega_0/2\pi$. Experimental results showing this relation are given in Fig. 2, where the frequency deviation $\Delta f=(p-\omega_0)/2$ is taken as the ordinate and the ratio of the signal power, P_1, to the output power of the test tube at its normal operation, P_0, as the abscissa. The entrained state can be realized in the region to the right of the curve. We

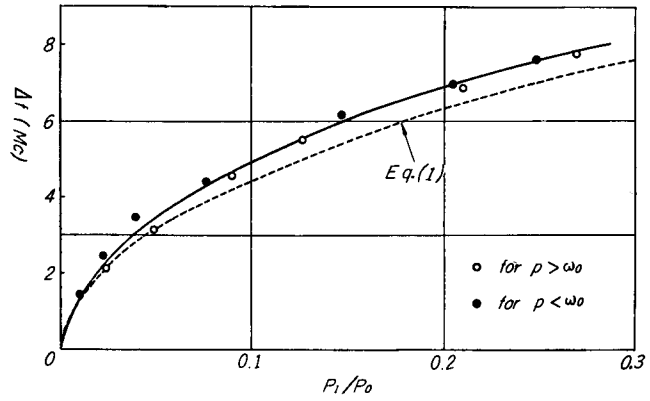

Fig. 2. Bandwidth of frequency entrainment versus signal power (when f_0=9036 Mc and cold test Q_{ext}=640). The theoretical curve based on Eq. (1) is plotted as a dotted line using cold test Q_{ext} of 640.

can learn from Fig. 2 how much bandwidth of frequency entrainment is obtained for a given P_1/P_0. It should be noted that the result of Fig. 2 agrees qualitatively with that predicted by the theory. The approximate formula theoretically derived for the bandwidth of entrainment is

$$\Delta f = \frac{f_0}{Q_{ext}}\sqrt{\frac{P_1}{P_0}} \quad (1)$$

in which $f_0=\omega_0/2\pi$ and Q_{ext} is the external Q of the klystron cavity.

In the above Δf was plotted versus P_1/P_0. In view of Eq. (1), it is also interesting to measure the Q_{ext}-dependence of Δf. Q_{ext} can be varied by changing the position of the shorting plunger of the klystron mount. For that purpose bandwidths of frequency entrainment under an adequate signal power were measured for various values of Q_{ext}. The results are shown in Fig. 3. The solid line in the figure was drawn using Eq. (1), and there is rough agreement with the measured values. It should be noted, however, that the values of Q_{ext} used in plotting the points are the cold test ones, which may differ appreciably from the true Q_{ext} values.

We have previously described the measurement of Δf for a klystron oscillator operating under the specified conditions initially mentioned, but it is also of interest to establish Δf versus P_1/P_0 curves for the following two cases:

(i) A lower voltage than

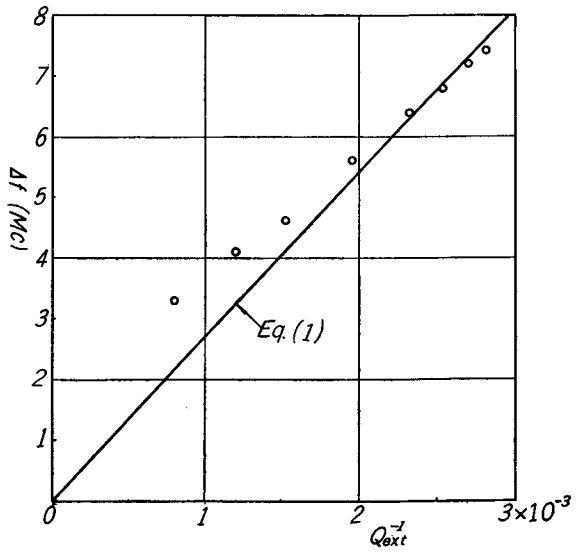

Fig. 3. Changes of Δf with Q_{ext}^{-1} (when f_0=9036 Mc and P_1/P_0=0.09). For plotting measured points, cold test values are used for Q_{ext}'s.

the standard value of the beam voltage is used.

(ii) The signal frequency p is held constant and ω_0 is varied by changing the repeller voltage or the beam voltage of the test tube. This case is of particular importance in connection with the attempt to amplify a signal of fixed frequency by use of the entrainment phenomenon.

The Δf measurements for these cases revealed almost the same results as Fig's 2 and 3, although no theoretical predictions for case (ii) have been given. Discussion of case (ii) will be given in a later section.

4. Output Power of an Entrained Klystron

Next we wish to inquire how the output power at the entrained state differs from that at normal operation. The net value of the output power, P_{out}, which flows out of the test tube was given in the previous paper by

$$\frac{P_{out}}{P_0} = \left(1+\frac{2V_0}{V}\sqrt{\frac{P_1}{P_0}}\cos\vartheta\right)\frac{V^2}{V_0^2} \qquad (2)$$

where V and V_0 are the amplitude of the gap voltage of the klystron cavity when entrained and at normal operation, respectively; $\vartheta-\pi$ is the phase difference between the signal and the cavity oscillation and depends both on $p-\omega_0$ and on P_1/P_0. The factor in parenthesis in Eq. (2) may be interpreted as an effective load conductance which is normalized by the characteristic admittance of the waveguide, the first term being the matched conductance and the second being an equivalent condudtance due to the applied signal.

P_{out} is given in terms of the measurable quantities by

$$P_{out} = P'_{out} - P_1 \qquad (3)$$

where P'_{out} is the power which is measured by the power meter II of Fig. 1. In Fig. 4a we plot the change of P'_{out}/P_0 with respect to P_1/P_0, becauce P'_{out} is the available power. For the case in which p is held constant at the value ω_a, the mode center value of the test tube, and ω_0 is varied by changing the repeller voltage of the klystron, Fig. 4b was obtained. Actually, in the case of both Fig. 4a and 4b some asymmetry was observed according as whether $p-\omega_0$ was positive or negative. But this asymmetry was ignored and the average of the two curves for $\pm|h|$ was plotted in these figures, where h is defined by $h=2(p-\omega_0)/\omega_0$.

The curves calculated from Eq. (2) are shown in Fig. 5a, which should be compared with Fig. 4a. Corresponding to Fig. 4b, Fig. 5b was drawn according to the analysis given in the following section. Qualitative agreement can be seen in both cases. The presence of the maximum of P'_{out} at $h=1.5\times10^{-3}$ in

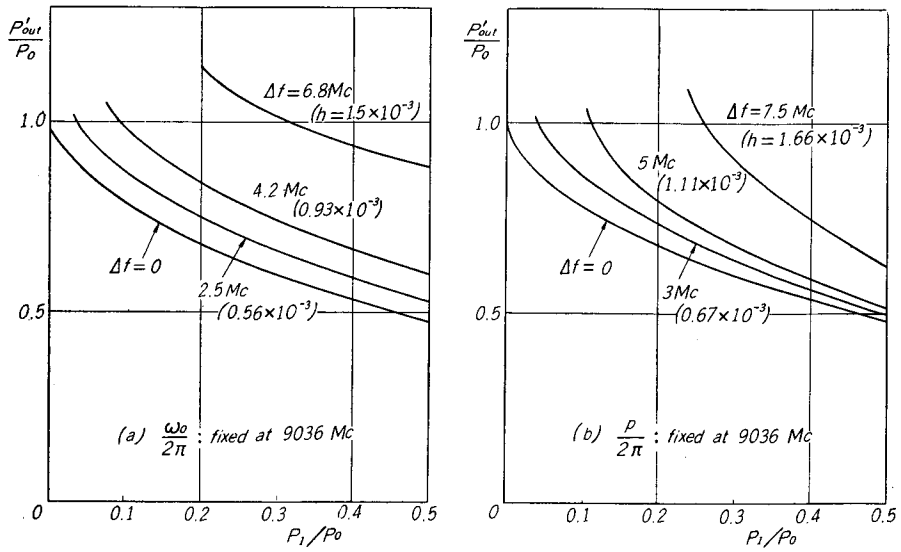

Fig. 4. Changes of P'_{out}/P_0 with P_1/P_0 for several $|h|$'s (when cold test $Q_{ext}=640$).

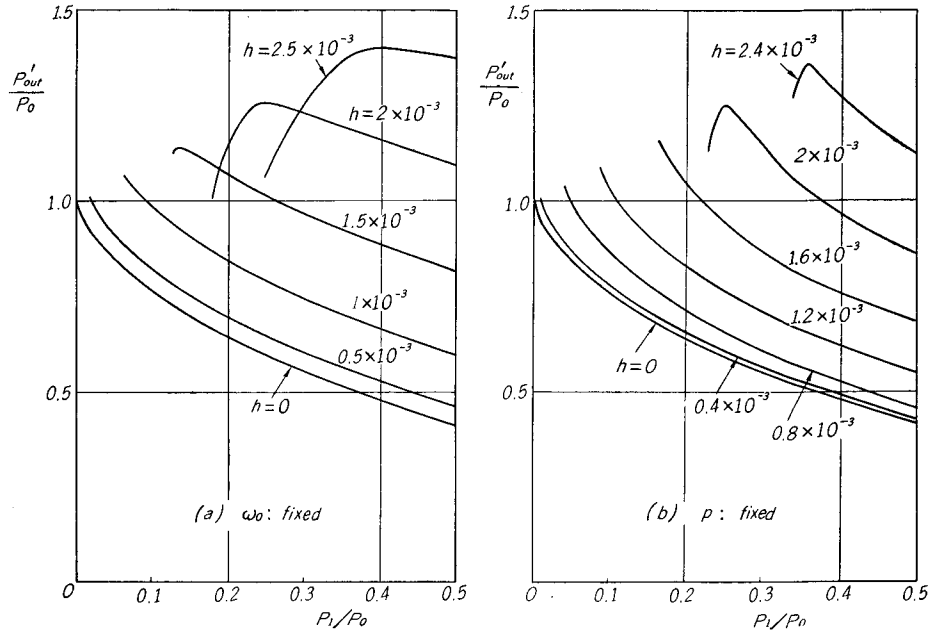

Fig. 5. Theoretical curves correspodding to Fig. 4.

Fig. 5a could not be observed because of a limitation in the magnitude of the signal power*, and partly because of fluctuations in the operational conditions of both the signal source and the test tube.

We can see from Fig. 4a or Fig. 5a that P'_{out} decreases with increasing P_1 for any $|h|$. This fact is not intrinsic with the entrainment phenomenon and will be referred to in the later part of this section.

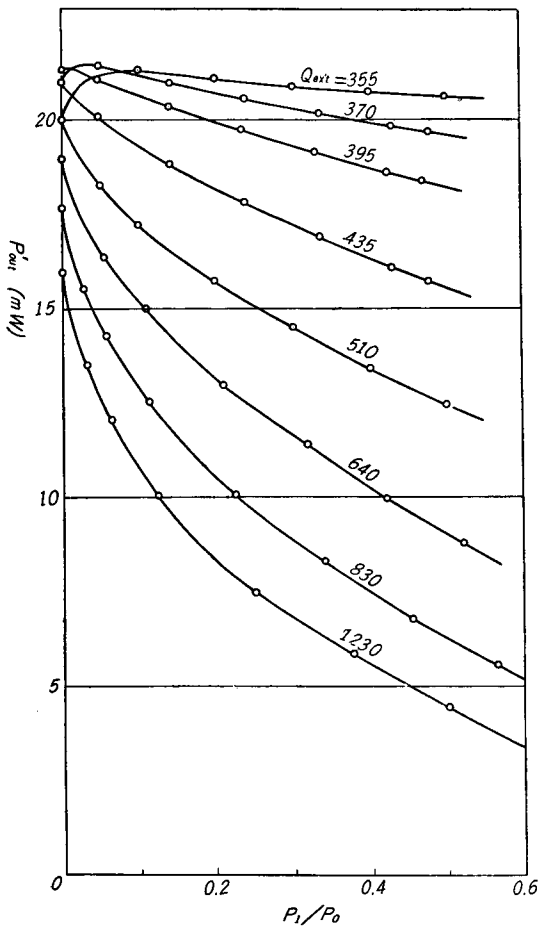

Fig. 6. Q_{ext}-dependence of P-P'_{out} curves (when $h=0$).

Next we must examine the Q_{ext}-dependence of the $P_1-P'_{out}$ curves. This was done for $h=0$ for simplicity and because the h-dependences of $P_1-P'_{out}$ curves for various Q_{ext}'s are something like as shown in Fig. 4a and 4b. First, it is seen from Fig. 6 that the stronger the output coupling (i.e. Q_{ext} decreases), the larger the value of P'_{out}/P_0 for any value of P_1/P_0. This may be interpreted as follows. Eq. (2) becomes for $h=0$

$$\frac{P_{out}}{P_0}=\left(1-\frac{2V_0}{V}\sqrt{\frac{P_1}{P_0}}\right)\frac{V^2}{V_0^2} \quad (4)$$

On the other hand, in the case $h=0$, we know that

$$\frac{V^2}{V_0^2}\left(\frac{V^2}{V_0^2}-1\right)^2 \propto \left(\frac{1}{P_0Q_{ext}}\right)^2\frac{P_1}{P_0} \quad (5)$$

from Eq. (4.19) of the previous paper. Then, for a given P_1/P_0, V/V_0 increases as Q_{ext} decreases. Thus P_{out}/P_0, and accordingly P'_{out}/P_0, increases with Q_{ext}^{-1} for a given P_1/P_0, because the two factors,

* For the circuit arrangement of Fig. 1, the maximum signal power obtained is about 0.25 of P_1/P_0. In Fig. 4, measurements at values of P_1/P_0 more than 0.25 were carried out in such a circuit arrangement that the T-junction II was removed and the branch waveguide was directly connected next to the variable attenuator. For this arrangement we have no means of identifying the occurrence of frequency entrainment, but it will at least be possible to extend the measurement made by the arrangement of Fig. 1 to values of P_1/P_0 greater than 0.25.

$\left(1-2\frac{V_0}{V}\sqrt{\frac{P_1}{P_0}}\right)$ and (V^2/V_0^2), both increase with increasing Q_{ext}^{-1}. Namely, in an entrained reflex klystron, both the effective load conductance and the gap voltage increase with increasing Q_{ext}^{-1}.

Another fact which is seen from Fig. 6 is that, as P_1/P_0 increases, P'_{out} increases in that range of P_1 for $Q_{ext}<Q_{ext,crit}$ and decreases monotonously for $Q_{ext}>Q_{ext,crit}$, where $Q_{ext,crit}$ lies near the value of Q_{ext} which gives the maximum output power at normal operation. This fact is easily interpreted because the rate of increase in the gap voltage exceeds the rate of decrease in the effective load conductance for $Q_{ext}<Q_{ext,crit}$. An analytical description of this fact may be given as follows. Writing Eq. (2) in terms of V^2,

$$\frac{P_{out}}{P_0}=\{1-\mu cQ_{ext}(V^2-V_0^2)\}\frac{V^2}{V_0^2}. \qquad (2)'$$

Now it is clear that if P_1 increases, so does V^2. Therefore, for the purpose of determining the sign of $\partial(P_{out}/P_0)/\partial(P_1/P_0)$, we may equally well examine the sign of $d(P_{out}/P_0)/d(V^2/V_0^2)$ in relation to the magnitude of Q_{ext}. It follows from Eq. (2)′ that

$$\frac{d(P_{out}/P_0)}{d(V^2/V_0^2)}=1-\mu cQ_{ext}(2V^2-V_0^2). \qquad (6)$$

Thus, if $Q_{ext}<(\mu cV_0^2)^{-1}$, then P_{out}/P_0 increases with P_1/P_0 for the range of P_1/P_0 which corresponds to $(\mu cQ_{ext})^{-1}+V_0^2>2V^2$. But if $Q_{ext}>(\mu cV_0^2)^{-1}$, then P_{out}/P_0 decreases with increasing P_1/P_0. The calculated value of $Q_{ext,crit}=(\mu cV_0^2)^{-1}$ is about 400 for the given experimental conditions, which is in fairly good agreement with the result of Fig. 6. Here it should be mentioned that this agreement holds generally for the values of h for which Eq. (1) is a good approximation.

5. Supplement to the Theory

In the theory previously presented the change in electronic susceptance, Δb, was ignored as compared with $2C(p-\omega_0)$. But, for discussing the case in which the normal operation of a reflex klystron is not at the center of an electronic mode, the effect of Δb must be considered. We will give a brief qualitative discussion about this point. All the notations used here are the same as in the previous paper.

For simplicity, our treatment in this section is confined to the case of matched loading. Assume that the initial operation point is at an electronic transit angle ϕ_0 from the mode center value. Then, assuming $\theta_0(p-\omega_0)/\omega_0\ll 1$, Δb can be written approximately as

$$\frac{\Delta b}{C\omega_a}\simeq\left(\frac{1}{Q_a}+\frac{1}{Q_{ext}}+\frac{A\cos\vartheta}{Q_{ext}}\right)\frac{p-\omega_0}{\omega_0}\theta_0\sec^2\phi_0+\frac{A\cos\vartheta}{Q_{ext}}\tan\phi_0. \qquad (7)$$

Note that, if ϕ_0 is fairly small and the first term in the right hand side of Eq. (7) is fairly large compared with the second term, Δb is of the same sign as the frequency deviation $p-\omega_0$.

Time variations of the amplitude of the gap voltage and of the phase retardation angle of the cavity oscillation from the applied signal are then expressed approximately as

$$2\frac{dV}{d\tau} = -\frac{\omega_a}{p}\{\mu c(V^2-V_0^2)V+E\cos\vartheta\} \equiv \Phi(V,\vartheta) \tag{8a}$$

$$2\frac{d\vartheta}{d\tau} = \frac{\omega_a}{p}\left[h\left\{1+\frac{1}{2}\left(\frac{1}{Q_a}+\frac{1}{Q_{\text{ext}}}+\frac{E\cos\vartheta}{V}\right)\theta_0\sec^2\phi_0\right\}+\frac{E}{V}(\sin\vartheta+\tan\phi_0\cos\vartheta)\right]$$
$$\equiv \Psi(V,\vartheta) \tag{8b}$$

in which A is replaced by

$$E = \frac{AV}{Q_{\text{ext}}}\left(=\frac{2V_0}{Q_{\text{ext}}}\sqrt{\frac{P_1}{P_0}}\right). \tag{9}$$

The electronic tuning range of a reflex klystron is usually limited to the range $\phi_0<\pi/3$. For ϕ_0's in this range, the second term in $1+\frac{1}{2}\left(\frac{1}{Q_a}+\frac{1}{Q_{\text{ext}}}+\frac{E\cos\vartheta}{V}\right)\theta_0\sec^2\phi_0$ in the right hand side of Eq. (8b) will, as in the case of $\phi_0=0$, be negligible as compared with 1.

Thus, neglecting that term, the stationary (entrained) state is given by

$$\mu c(V^2-V_0^2)V+E\cos\vartheta = 0 \tag{10a}$$

$$hV+E(\sin\vartheta+\tan\phi_0\cos\vartheta) = 0. \tag{10b}$$

Note that the first of these equations has the same form as in the case of $\phi_0=0$. Let the notations V and ϑ be used in the following to denote the solutions of Eqs. (10a) and (10b). Eliminating ϑ from these equations and using the approximate relation $\mu c=\alpha/V_0^2$, we have

$$\left\{\alpha^2\left(\frac{V^2}{V_0^2}-1\right)^2\sec^2\phi_0-2\alpha h\left(\frac{V^2}{V_0^2}-1\right)\tan\phi_0+h^2\right\}\frac{V^2}{V_0^2} = \frac{E^2}{V_0^2}. \tag{11}$$

From this equation the $h-V^2$ diagram can be drawn, E being taken as a parameter. The stable region in the $h-V^2$ plane is known to be determined by the conditions:

$$P = -\{\Phi_{V'}(V,\vartheta)+\Psi_{\vartheta'}(V,\vartheta)\}>0$$

and

$$Q = \begin{vmatrix}\Phi_{V'}(V,\vartheta) & \Phi_{\vartheta'}(V,\vartheta)\\ \Psi_{V'}(V,\vartheta) & \Psi_{\vartheta'}(V,\vartheta)\end{vmatrix}>0.$$

These conditions become, in our case,

$$\frac{V^2}{V_0^2} > \frac{\tan\phi_0}{\alpha(4+\tan^2\phi_0)}h + \frac{2+\tan^2\phi_0}{4+\tan^2\phi_0} \tag{12a}$$

$$9\left(\frac{V^2}{V_0^2}-\frac{2}{3}\right)^2 - \frac{6\sin 2\phi_0}{\alpha}\left(\frac{V^2}{V_0^2}-\frac{1}{2}\right)h + \frac{3\cos^2\phi_0}{\alpha^2}h^2 > 1. \tag{12b}$$

The condition (12b) represents the area outside of an ellipse in the $h-(V^2/V_0^2)$ plane which, as in the case of $\phi_0=0$, intersects the V^2/V_0^2 axis at 1 and 1/3. The sketches of the $h-(V^2/V_0^2)$ relations for the case $\phi_0 \neq 0$ are given in Fig. 7.

Now a rough estimate of the bandwidth of frequency entrainment for a given strength, E, of external force can be done in a similar way to the case of $\phi_0=0$. For a small E, as is seen from Fig. 7, the stable region can roughly be

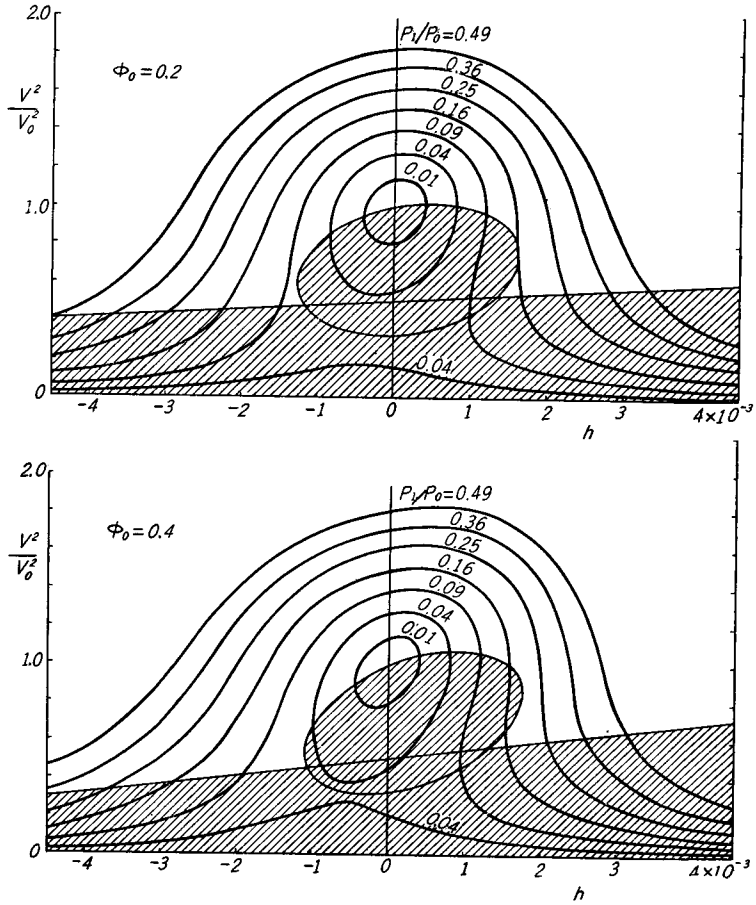

Fig. 7. h–V^2 diagrams for the cases $\phi_0=0.2$ and 0.4. As a parameter P_1/P_0 is used instead of E. The hatched regions correspond to unstable states. These diagrams are drawn for the assumed valnes: $Q_a=Q_{ext}=500$, $X=1.84$ (when $\phi_0=0$), $M^2=0.5$, $n=2$, $V_b=300$ and $\nu=0.1058$.

regarded as the upper part of the tangential line to the ellipse at $h=0$ and $V^2/V_0^2=1$. The equation of this tangential line is

$$\frac{V^2}{V_0^2}=1+\frac{\sin 2\phi_0}{2\alpha}h. \tag{13}$$

The maximum frequency deviation within which the frequency entrainment should occur by an external force of strength E can be determined from the positive root, $h_{\max}^{+}$, and the negative root, $h_{\max}^{-}$, having a smaller absolute value, from the following equation:

$$h^2\left(1+\frac{\sin 2\phi_0}{2\alpha}h\right)=\frac{E^2}{V_0^2}\sec^2\phi_0. \tag{14}$$

From Eq. (14), it is seen that (i) $h_{\max}^{+}$ is smaller or larger than $h_{\max}^{-}$ according as $\phi_0>0$ or $\phi_0<0$, and (ii) the difference between the two becomes marked as $|\phi_0|$ increases. When $|\phi_0|$ is fairly small and

$$(E/V_0)|\sin\phi_0|\ll\alpha, \tag{15}$$

then $|h_{\max}|=(E/V_0)\sec\phi_0$ and we shall have almost the same bandwidth as in the case $\phi_0=0$. Here we may inquire how small ϕ_0 should be in order to satisfy condition (15) when $P_1/P_0=0.1$. Under a typical operational condition, we have $\alpha\simeq(6.5\cos\phi_0-4)\times10^{-3}$ and $(E/V_0)=1.2\times10^{-3}$ for $P_1/P_0=0.1$. Inequality (15) then holds as far as $\phi_0\lesssim0.2$. For a 10*Gc*-band reflex klystron, this corresponds to a 4*Mc* distance from the mode center frequency.

Next, we will consider the P_1-P_{out} relations. Expressions (2) and (2)′ still hold in the case $\phi_0\neq0$, too. So we have, using Eqs. (6) and (11),

$$\begin{aligned}\frac{\partial(P_{\text{out}}/P_0)}{\partial(P_1/P_0)}&=\left(\frac{2}{Q_{\text{ext}}}\right)^2\frac{d(P_{\text{out}}/P_0)}{d(V^2/V_0^2)}\frac{\partial(V^2/V_0^2)}{\partial(E^2/V_0^2)}\\&=\left(\frac{2}{Q_{\text{ext}}}\right)^2\frac{1-\alpha Q_{\text{ext}}\left(\frac{2V^2}{V_0^2}-1\right)}{\alpha^2\left(\frac{3V^2}{V_0^2}-1\right)\left(\frac{V^2}{V_0^2}-1\right)\sec^2\phi_0-2\alpha h\left(\frac{2V^2}{V_0^2}-1\right)\tan\phi_0+h^2}.\end{aligned} \tag{16}$$

This equation may be used for a qualitative discussion about the slope of the P_1-P_{out} curves. For instance, if we make the denominator of the right hand side of Eq. (16) zero, the resultant equation proves to be just the ellipse $Q=0$. This means that the P_1-P_{out} curve begins with an infinite slope, which takes either a positive or negative sign according to the value of Q_{ext}. We saw already in Figs. 4 and 6 that this was the case.

The experimental results of Fig. 4b cannot be explained by mere inspection of the relations given above. But the calculation which is carried out using Eqs. (2) and (11) and the relations

$$h = \left(\frac{1}{Q_a} + \frac{1}{Q_{ext}}\right) \tan \phi_0 ,$$

gives a satisfactory explanation of the experimental results as was stated before.

6. Conclusions

It can be said from the arguments in the foregoing sections that the theory gives at least a qualitative explanation of the experimental results. More precise comparison between theory and experiment was impossible because of the following factors: (1) the theory presented is based on the simple klystron theory and cannot distinguish the differences due to whether h is positive or negative, (2) we cannot know the correct Q_{ext} values at operating conditions.

Descriptions of the static part of the phenomenon may be covered if measurements of the phase retardation of the cavity oscillation of a frequency-entrained klystron from the applied signal were carried out, but this was left for future study.

From a practical point of view, the results of Fig. 6 may be rather noteworthy. If more power is desirable, Q_{ext} should be chosen at a value somewhat smaller than the value which gives the maximum output power at self-excited oscillation.

References

1) J. C. Slater; "Microwave Electronics", D. Van Nostrand Co., Inc., New York (1950).
2) J. Ikenoue and K. Fukui; THIS MEMOIRS, **22**, 197 (1960).